

Functionalization of Graphite Electrodes with Aryl Diazonium Salts for Lithium-Ion Batteries

Marina Bauer, Kristina Pfeifer, Xianlin Luo, Hannes Radinger, Helmut Ehrenberg, and Frieder Scheiba*^[a]

The functionalization of electrode surfaces is a useful approach to gain a better understanding of solid–electrolyte interphase formation and battery performance in lithium-ion batteries (LIBs). Electrografting and deprotection of alkyl silyl protected ethynyl aryl diazonium salts on graphite electrodes were performed. Furthermore, electrografting of aryl diazonium salts carrying functional groups such as amino, carboxy and nitro, and their influence on the electrochemical performance in LIBs were investigated. The drawbacks of electrografted and

especially deprotected samples were evaluated and compared to corresponding *in situ* grafted samples. While electrografted samples tend to lower the delithiation capacities, *in situ* grafted samples, except amino groups, reveal higher capacities. Ethynyl (TMS) shows improved capacities at 1 C and better capacity retention compared to the pristine graphite electrode. Additionally, the Coulombic efficiency of the first cycle was enhanced for *in situ* grafted samples.

Introduction

Up to date, graphite is still the most commonly used anode material in commercial lithium-ion batteries (LIBs).^[1–3] The formation of a so-called solid electrolyte interphase (SEI) on the surface of the graphite electrode determines the cycling stability of LIBs. The SEI forms during the first few cycles due to electrolyte decomposition at low potentials (< 1 V vs. Li^+/Li).^[4] Modifying the surface of the active material is a promising approach to introduce certain functionalities to understand how different surface groups affect the SEI formation and hence battery performance.^[5]

The grafting of aryl diazonium salts (ADS) to a variety of surfaces, including carbon-based materials has been extensively studied.^[6–12] Leroux and Hapiot^[13] reported that the grafting density of electrografted ethynyl diazonium salts on glassy carbon can be tuned by varying the size of the protecting group. Further, they found that a trimethylsilyl (TMS) protecting group is already bulky enough to prevent multilayer formation. Grafting of ADS has already been used to modify graphite electrodes in LIBs. In a previous work, Moock *et al.*^[14] successfully electrografted and deprotected a TMS protected ethynyl ADS on a graphite electrode. They achieved enhanced capacity and cycling stability compared to a graphite-based reference

system. Pan *et al.*^[15] accomplished enhanced capacity and cycling stability for graphite electrodes in LIBs by grafting a nitro ADS to graphite powder. In another study by Verma and Novák,^[16] different grafting methods of a carboxy ADS were investigated. They found that aqueous *in situ* grafting leads to thinner surface layers compared to electrografting, which are advantageous to retain capacity and cycling stability in the battery. This study demonstrates that the grafting method must be considered to evaluate the influence of functional groups on the performance of the cell.

Although these findings have proved successful modifications of graphite electrodes with ADS and partly enhanced the electrochemical performance in LIBs, the results must be adapted to application-oriented electrode systems in terms of the electrode composition. Comparing the impact of different grafting methods and functional groups of ADS with the literature is difficult since different graphitic materials and binders were used in different cell types and setups. In the state-of-the-art literature, the electrodes consisted of 90% w/w graphite as active material and 10% w/w binder. Commercial electrodes additionally contain a conductive carbon additive (usually < 10 % w/w)^[17] to achieve better particle-particle contact and guarantee sufficient electron conductive pathways in the electrode.^[18–20] For example, Moock *et al.*^[14] presented an electrode, which lost 44% of its initial capacity after only ten cycles at C/20, but commercial graphite electrodes can withstand more than 1000 cycles. Adding conductive additive could already lead to improved capacity and cycling stability of the used graphite electrodes. The influence of ADS modifications on realistic graphite electrode compositions remains to be evaluated. Furthermore, Pan *et al.*^[15] and Verma and Novák^[16] used a two-electrode graphite/lithium metal setup for electrochemical cycling. A three-electrode cell setup is more precise as the processes on the Li-metal are excluded and will not superimpose the effects originating from the grafted surface groups. Besides electrode composition and cell setup, the

[a] M. Bauer, Dr. K. Pfeifer, X. Luo, H. Radinger, Prof. Dr. H. Ehrenberg, Dr. F. Scheiba
Institute for Applied Materials
Karlsruhe Institute of Technology
Hermann-von-Helmholtz-Platz 1, 76344 Eggenstein-Leopoldshafen, Germany
E-mail: frieder.scheiba@kit.edu

Supporting information for this article is available on the WWW under <https://doi.org/10.1002/celec.202101434>

© 2021 The Authors. ChemElectroChem published by Wiley-VCH GmbH. This is an open access article under the terms of the Creative Commons Attribution License, which permits use, distribution and reproduction in any medium, provided the original work is properly cited.

charge/discharge current for electrochemical measurements varies from C/20 to C/10. The performance at higher currents is not investigated at all.

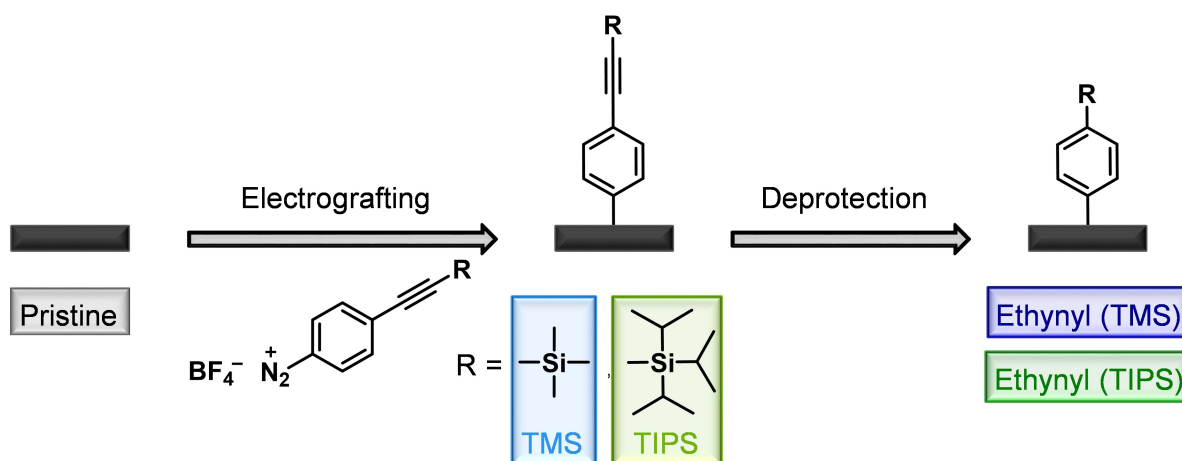
However, Moock *et al.*,^[14] Pan *et al.*^[15] and Verma and Novák^[16] provide useful information about the relation of diazonium phenyl grafted graphite and their electrochemical performance in LIBs in their particular experiments. What these works do not reveal, is if these findings are applicable to a uniform experimental setup and still show the same effects. For example, do hydrophilic groups perform better than hydrophobic? Is the choice of the grafting method crucial for groups other than carboxy as well? Or are reduced functional groups advantageous in general? In order to provide comparable values to these questions, we investigated electro- and *in situ* grafting of ethynyl (hydrophobic, reducible), amino (hydrophilic, not reducible), carboxy (hydrophilic, reducible) and nitro groups (hydroneutral, reducible) to better understand the effects of grafted ADS on electrochemical performances of graphite electrodes for LIBs. Ethynyl groups are protected with an alkyl silyl protecting group for the grafting step. To determine whether the distance between deprotected ethynyl groups is of importance, two different sized alkyl silyl protecting groups are under study for electrografting experiments. The surface composition and morphology were studied using X-ray photoelectron spectroscopy (XPS) and scanning electron microscopy (SEM). The electrochemical performance was evaluated using a three-electrode setup with realistic electrode composition. The influence of the grafting method and the corresponding influence of each functional group are addressed.

Results and Discussion

Electrografting of alkyl silyl protected ethynyl aryl diazonium salts

Graphite electrodes were used as substrates for electrografting experiments according to a method displayed in Scheme 1. The electrografted electrodes are referred to as TMS and TIPS,

whereas the deprotected electrodes are labelled as ethynyl. To distinguish the ethynyl groups from each other, the protecting group from which they derived is added in brackets, giving ethynyl (TMS) and ethynyl (TIPS). Silicon in alkyl silyl protecting groups works as a marker to confirm successful electrografting via XPS (Figure 1a). The appearance of Si 2p peaks at a binding energy of 100.5 eV (Si 2p_{3/2}) in TMS and TIPS corresponding to silicon linked to carbon suggests that the electrografting of the protected ethynyl moiety was performed successfully.^[14] The silicon content for TMS (3.2 at%) is higher than for TIPS (1.4 at%), which is attributed to the higher distance between the molecules caused by the more steric demanding TIPS group. As expected, Si 2p peaks in ethynyl (TMS) and ethynyl (TIPS) disappeared after the deprotection of the ethynyl moiety. The SEM images of the reference and all modified electrodes (Figure 1b) show conductive additive particles and a fibrous structure on the graphite surface of the pristine, TMS and TIPS samples, which is assigned to the PVdF binder.^[21] However, in the images of ethynyl (TMS) and ethynyl (TIPS) additional spots are visible on the electrode surface, whereas ethynyl (TMS) shows visibly more spots than ethynyl (TIPS). The spots most probably evolve during the deprotection process. To investigate the electrochemical performance of ethynyl (TMS) and ethynyl (TIPS) compared to the pristine electrode, a three-electrode setup was used. The electrochemical cycling performance and Coulombic efficiencies are presented in Figures 1c and d, respectively. The delithiation capacities decrease for the modified samples at low rate, whereas constant capacity values are observed for the pristine graphite electrode (Figure 1c). A massive drop in capacity from 335 mAhg⁻¹ to 97 mAhg⁻¹ appears for the modified samples when applying a higher current. This drop (71%) is much higher than for the pristine (28%), which gives reason to assume slower intercalation kinetics due to blocked intercalation channels for the modified electrodes. Moreover, the ethynyl (TIPS) values at 1 C fluctuate, indicating inhomogeneous SEI formation, which may be attributed to the creation of "pinholes" on the surface as described in literature.^[13] In addition, efficiencies in the first cycle of both samples noticeable dropped by 10% compared to



Scheme 1. Electrografting of alkyl silyl protected ethynyl aryl diazonium salts to graphite electrodes.

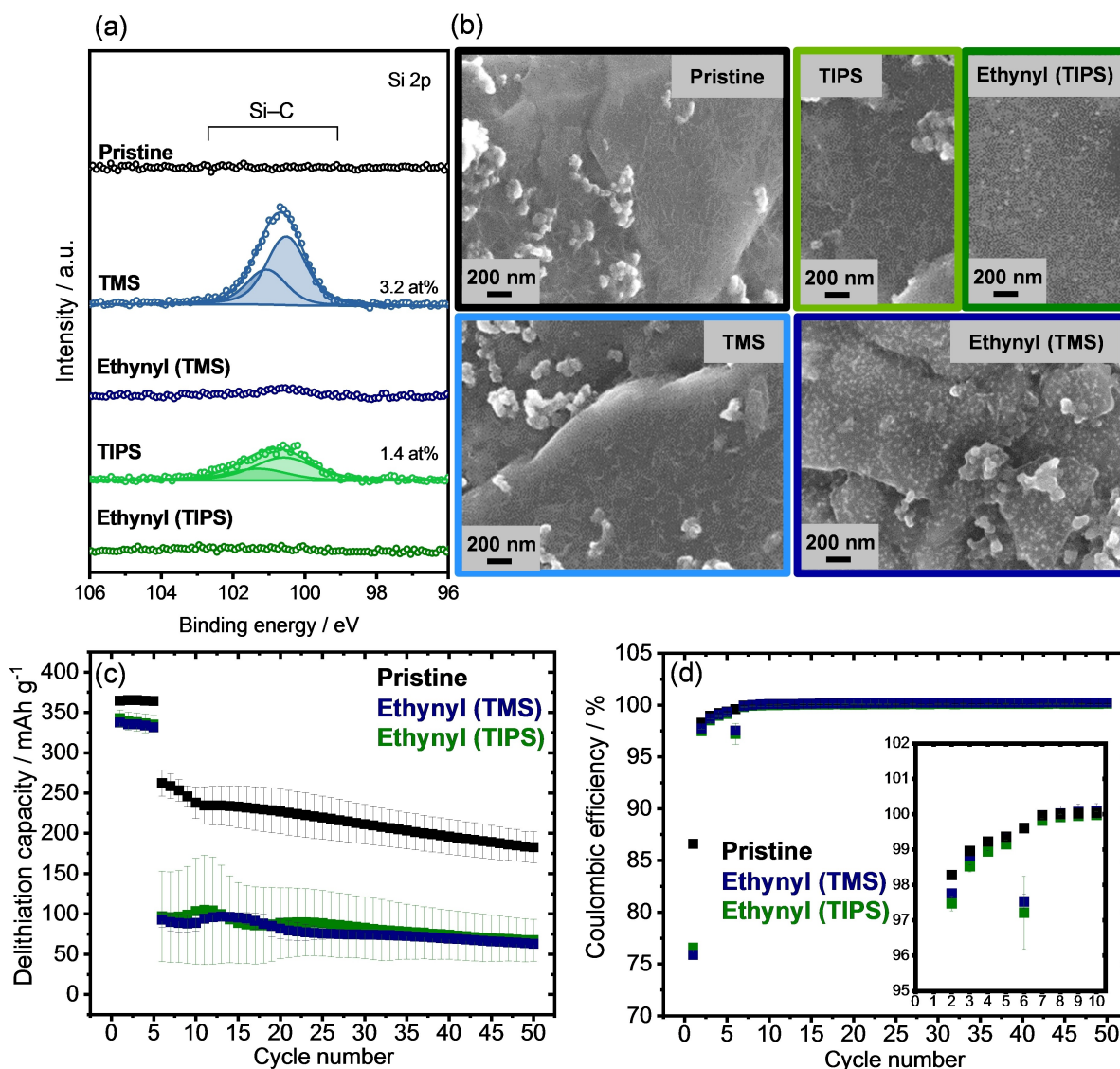


Figure 1. (a) Si 2p spectra and (b) SEM images of pristine, electrografted and deprotected electrodes; (c) electrochemical cycling stability at C/10 for 5 cycles and 1 C for 45 cycles and (d) corresponding Coulombic efficiencies of the pristine and deprotected electrodes.

pristine, indicating more irreversible side reactions during the first lithiation (Figure 1d). Although, the difference in efficiencies at C/10 compared to the pristine is not as drastic as in the first cycle, the consumption of lithium-ions due to side reactions is more distinct for the modified samples (Figure 1d, inset). We assume that the formed SEI is not stable, as side reactions proceed even after 5 cycles. However, after two cycles at 1 C the efficiencies are comparable to the pristine electrode.

We investigated whether the spots appearing on the surfaces of ethynyl (TMS) and ethynyl (TIPS) could also contribute to the poor performance. Therefore, a pristine electrode and bare graphite powder were treated with the deprotection agent (TBAF 0.1 M in THF) and characterized by SEM (Figure 2a). Since the surface of treated graphite powder is free from spots but the treated electrode is not (Figure 2a), the spots originate from a decomposition of the PVdF binder. To further investigate this phenomenon, we conducted XPS measurements of pristine PVdF powder and PVdF treated with

deprotection agent. Figure 2b shows the C 1s and F 1s XPS spectra of the two corresponding powders. The C 1s regions were deconvoluted into four peaks: C–C/C–H at 285.0 eV, CH₂/C–O at 286.6 eV, COO/CHF at 288.5 eV and CF₂ at 290.9 eV.^[22] CH₂ and CF₂ refer to the bonds in PVdF, of which the intensities drastically decrease after treatment with TBAF. The peak in the F 1s region at around 687.9 eV represents CF₂ in PVdF, which decreased after deprotection. Moreover, two additional peaks at 683.8 eV for fluoride and 686.1 eV for CHF can be observed for the deprotected sample. C 1s and F 1s spectra of the corresponding electrodes can be found in Figure S1. It is notable that during the preparation of the PVdF (TBAF) sample, we observed that the originally white PVdF powder immediately turns to black when immersed in the deprotection agent (Figure S2). This observation and the XPS results confirm our assumption that side reactions occurred when the PVdF containing electrode was treated with deprotection agent. This

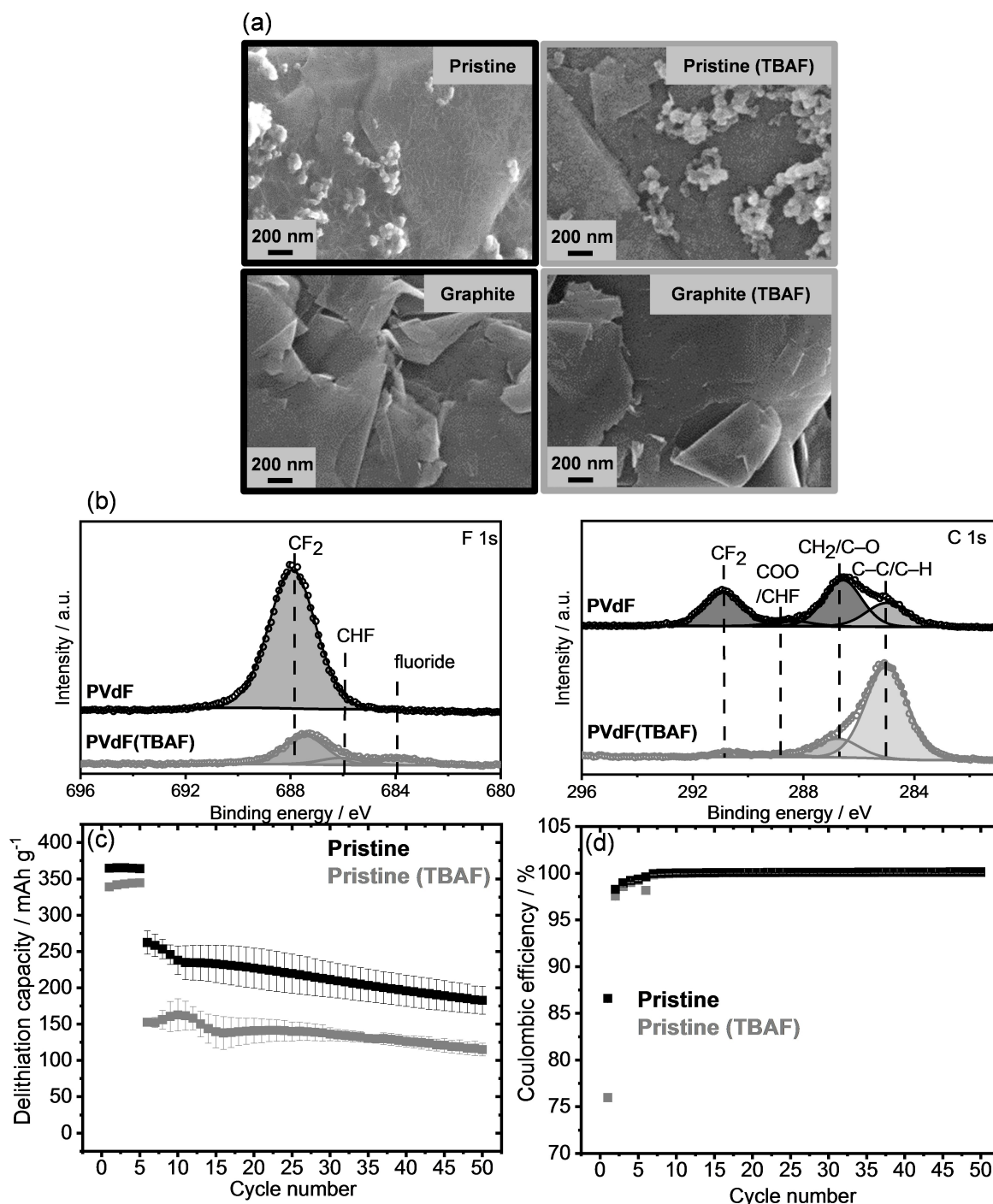


Figure 2. (a) SEM images of pristine and with TBAF treated graphite electrode and graphite powder; (b) C 1s and F1s spectra of pristine and with TBAF treated PVdF binder; (c) electrochemical cycling stability at C/10 for 5 cycles and 1 C for 45 cycles and (d) corresponding Coulombic efficiencies of pristine and with TBAF treated graphite reference electrode.

is in line with the electrochemical results demonstrated in Figure 2c–d. The graphite electrode, which was solely treated with TBAF exposes a decrease of delithiation capacity and efficiency in the first cycle in comparison to the pristine electrode. These observations point out that a treatment with TBAF causes a visible change of the electrode surface and decomposition of the binder, resulting in poor electrochemical performance. The effect of binder decomposition could likely

affect the impact of the grafted surface groups. To avoid side reactions with PVdF, all experiments were repeated using CMC/SBR instead of PVdF. However, SEM and XPS reveal decomposition of CMC binder most likely due to deacylation after treatment with deprotection agent,^[23] which negatively influences the electrochemical performance of the electrodes as well (Figures S3–S4). Since the role of the binder is to ensure good particle-particle cohesion and particle-current collector adhe-

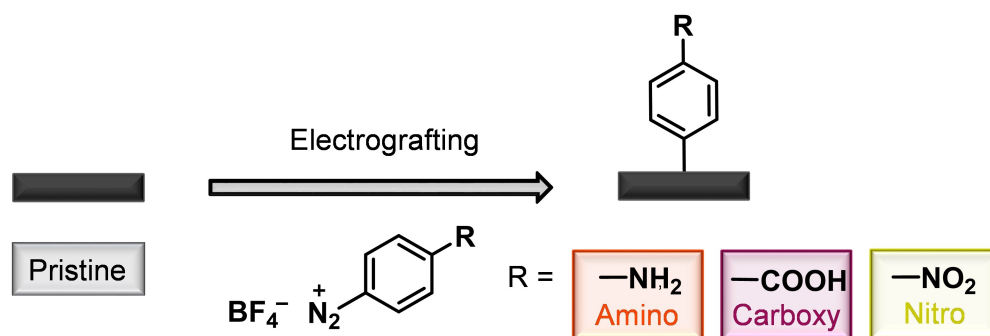
sion to enable stable cycling, it is not surprising that binder decomposition results in poor electrochemical performance. Nonetheless, capacities of ethynyl (TMS) and ethynyl (TIPS) are even lower compared to the TBAF treated pristine electrode, which proposes an additional influence of the electrografting process and/or the ethynyl functionality. Therefore, additional functional groups were investigated.

Electro- and in situ grafting of functionalized aryl diazonium salts

To avoid binder decomposition by a deprotecting agent, ADS with amino, carboxy and nitro moieties were electrografted to graphite electrodes (Scheme 2). The electrografted samples are referred to as amino, carboxy and nitro. In this case, no secondary deprotection step is needed after grafting. Surface analyses *via* XPS and SEM are displayed in Figure S5. The characteristic N 1s peaks for amino and nitro groups as well as O 1s peaks for carboxy groups confirm successful grafting of the salts. Looking at the influence of these groups on the electrochemical behavior, it can be seen that all electrografted samples show reduced delithiation capacities, especially at a higher current (Figure 3a). Even though the electrodes were not

treated with an additional deprotecting agent, the capacities are not improved compared to Ethynyl (TMS) and Ethynyl (TIPS). A reasonable explanation for this behaviour is the radical mechanism of electrografting.^[24] Due to the absence of a protecting group, the formation of dense multilayers is more likely, which may block the graphite surface and hinders lithium-ion intercalation. The thick layer could also inhibit electrolyte penetration and change the porosity of the electrode and therefore lead to lower capacities.^[25] The initial capacity loss for carboxy and amino are close to the pristine electrode, whereas it increases for nitro (Figure 3b). The efficiencies of amino in the following cycles are similar to the pristine and nitro. Especially carboxy shows reduced efficiencies at C/10. After the current change, amino and nitro show efficiencies similar to the pristine, whereas for carboxy the efficiencies are still below the pristine after 10 cycles. The addition of functional groups *via* electrografting is expected to lead to a more reactive surface, which would promote more side reactions upon cycling, especially for reducible functional groups.^[16]

To preserve free intercalation channels, another modification method was tested. Functionalized aryl anilines were mixed with diazotization reagent and graphite powder in an acidic aqueous solution. Since the corresponding ADS are *in situ*



Scheme 2. Electrografting of amino, carboxy and nitro aryl diazonium salts to graphite electrodes.

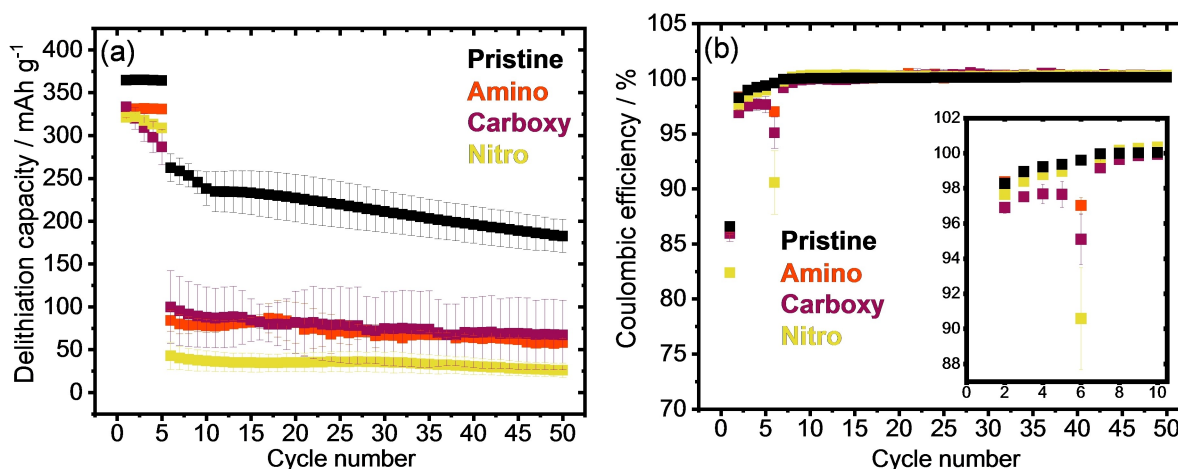


Figure 3. (a) Electrochemical cycling stability at C/10 for 5 cycles and 1 C for 45 cycles and (b) corresponding Coulombic efficiencies of pristine and electrografted amino, carboxy and nitro electrodes.

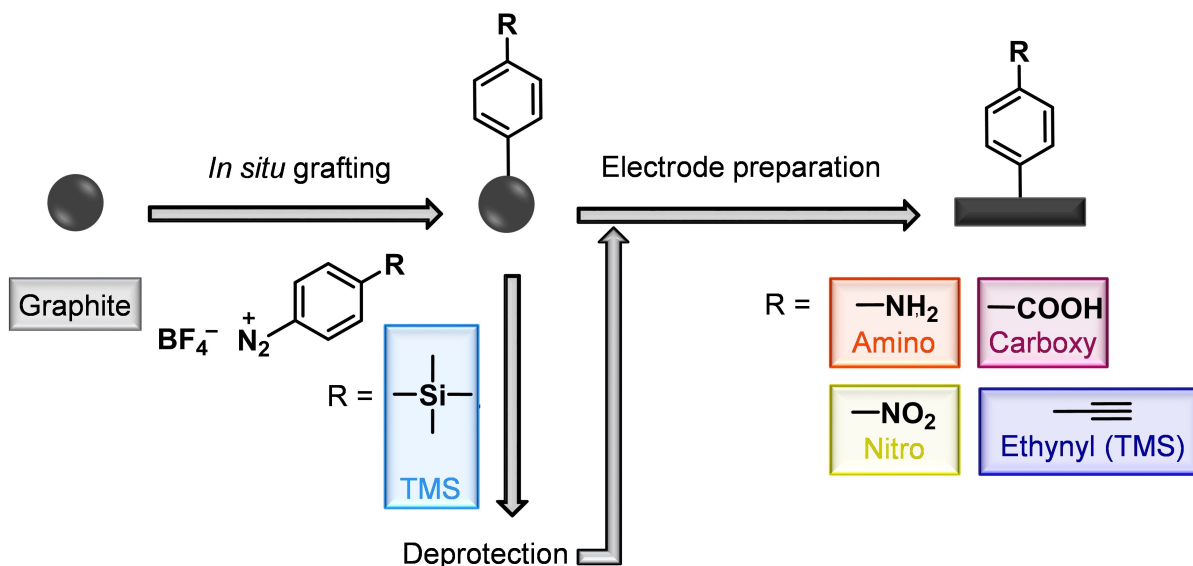
formed and grafted to the graphite powder, this method is referred to as *in situ* grafting (Scheme 3).^[26] Since for *in situ* grafting the graphite powder is modified before the preparation of the electrode, deprotection of TMS can be done without decomposition of the binder. The resulting electrodes are referred to as TMS, ethynyl (TMS), amino, carboxy and nitro. Again, the appearance of a Si 2p peak for TMS and subsequent disappearance after deprotection confirms successful grafting via the *in situ* method (Figure 4a). For the amino and nitro groups, nitrogen works as marker molecule. The N 1s peak of amino which is observed after *in situ* grafting was fitted with two components of $-N<$ at 399.3 eV^[27] and $N=$ at 400.7 eV.^[27] For the Nitro sample, an additional N 1s peak at 405.7 eV^[28] corresponding to $-NO_2$ appears as expected. For Carboxy, both O 1s spectra were deconvoluted by a peak of COO at lower binding energy and a peak of C–O at higher binding energy. Despite the shift in binding energy due to the charging effect, the intensity of COO and C–O peaks increased after *in situ* grafting, indicating that the electrode was successfully modified.

None of the *in situ* grafted samples shows the fiber-like structure of PVdF in the SEM images (Figure 4b). Carboxy shows a morphology similar to the pristine, whereas ethynyl (TMS), nitro and amino look like they are covered by a film, which supports that multilayer formation also occurs by using this method (Figure 4b). However, the spots observed for electrografted ethynyl (TMS) do not appear for *in situ* grafted ethynyl (TMS), which confirms the side reactions of TBAF with PVdF.

Compared to the electrografted samples, *in situ* grafted samples, except amino, show higher delithiation capacities, (Figure 5a). Amino shows a drastic capacity decrease and delivers almost no capacity at higher current, hence, the Coulombic efficiency of $>100\%$ is not meaningful, as the material is not electrochemically active anymore and the charge transfer cannot be attributed to electrochemical storage processes. The very low capacity (less than 13 mAhg^{-1}) stems

from capacitive storage which in this case is not regular. Amino groups being activating substituents may cause different grafting behaviour and different electrochemical performance. The capacity of the carboxy sample is comparable to the pristine sample. Ethynyl (TMS) has still a higher capacity (245 mAhg^{-1}) and cycling stability than the pristine (238 mAhg^{-1}) after ten cycles. This trend is preserved up to 45 cycles with a capacity retention of 84% for ethynyl (TMS) compared to 70% for the pristine. This means that fewer lithium-ions are consumed for SEI formation and are therefore further available for (de)intercalation. However, at C/10 the capacities drop after the first cycle, due to an increase of side reactions. Even though the efficiencies in the first cycle are higher than for the pristine, this trend changes in the following cycles at low current (Figure 5b). This was also noted for electrografted samples and attributed to increased reactivity of the surface due to an incorporation of functional groups.

SEI formation includes the reduction of electrolyte components and subsequent precipitation of decomposition products on the electrode's surface.^[29] *In situ* grafted samples show the presence of the ethylene carbonate (EC) reduction peak at $\sim 0.8 \text{ V}$ ^[30] (except amino), whereas this peak is suppressed or even absent for electrografted samples (Figure 6a,c,d, insets). Despite the consumption of lithium-ions during EC reduction, the *in situ* grafting increased the initial Coulombic efficiency for nitro (88%), carboxy (89%) and ethynyl (TMS) (90%) compared to electrografted analogues (82%, 86% and 76%, respectively) and also slightly compared to the pristine graphite (87%). It is well known that additives like vinylene carbonate (VC) stabilize the SEI due to polymerization effects.^[31] It is likely that triple bonds polymerize as well and therefore influence the properties of the SEI, which can be observed for ethynyl (TMS). We expect that the polymerization is not finalized during the low rate cycling, but already sufficiently developed to enhance the performance at high rates. We do not observe an enhanced rate capability for the electrografting process as the groups are



Scheme 3. *In situ* grafting of amino, carboxy, nitro and ethynyl (TMS) aryl diazonium salts to graphite electrodes.

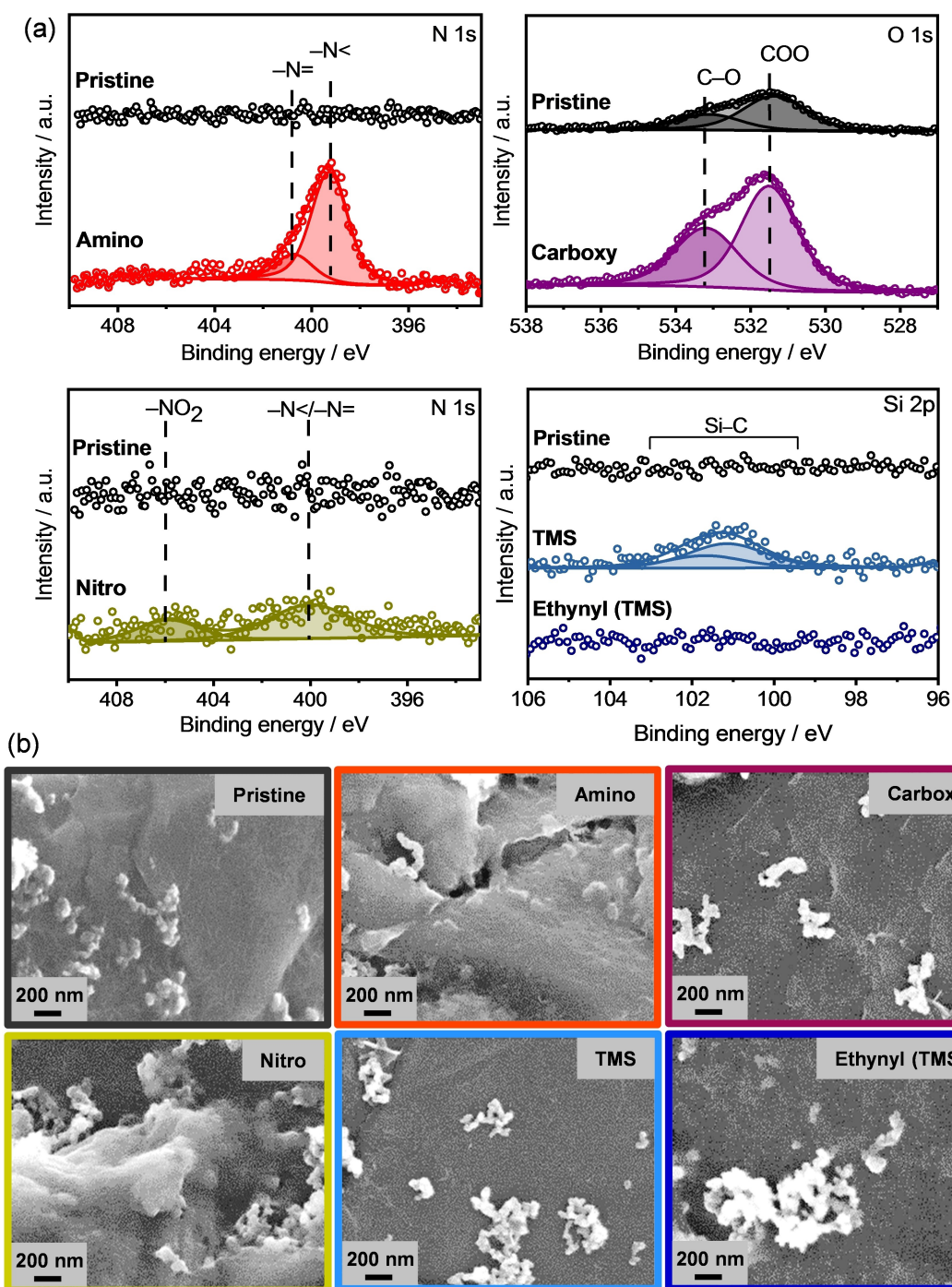


Figure 4. (a) N 1s, O 1s and Si 2p spectra and (b) SEM images of pristine, *in situ* grafted (and deprotected) electrodes.

probably arranged too dense and therefore inhibit the insertion of lithium-ions.

Differential capacity plots of the first cycle (Figure 6a) additionally show that the lithium-ion transport is much more affected by ethynyl (TMS) than ethynyl (TIPS), given that the reduction peaks are broadened and shifted to lower potentials. After removing the protecting group, there is no difference in the chemical structure of ethynyl (TMS) and ethynyl (TIPS), but the amount of ethynyl groups on the surface is higher for

ethynyl (TMS). The rigidity of the dense grafted ethynyl groups and the resulting network during reduction seems to alter the lithium-ion transport. This effect is attenuated if the ethynyl groups are grafted less dense as in ethynyl (TIPS). However, the transport during oxidation is also affected by ethynyl (TIPS) in a similar manner as by ethynyl (TMS), which means the ethynyl group and the resulting decomposition products affect lithium-ion transport in general for samples prepared by the described

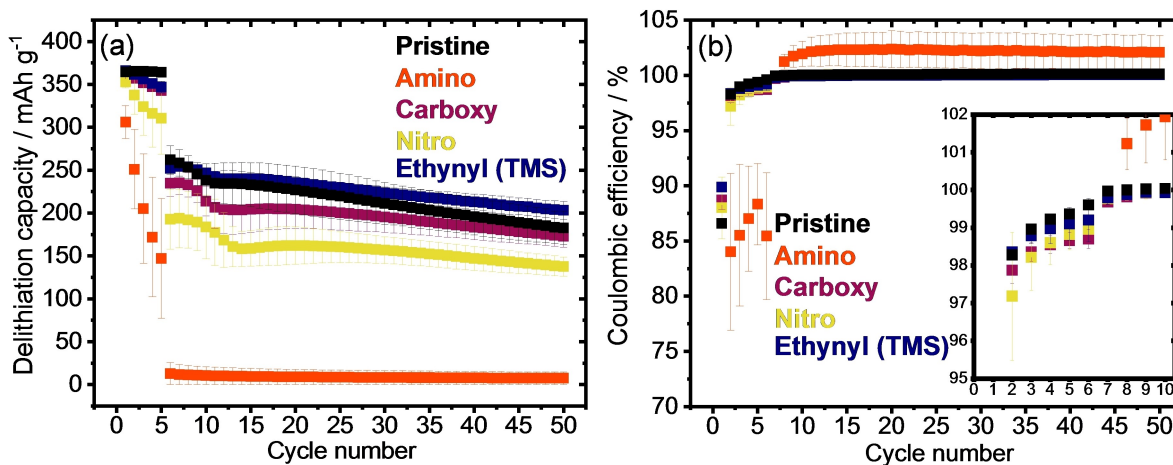


Figure 5. (a) Electrochemical cycling stability at C/10 for 5 cycles and 1 C for 45 cycles and (b) corresponding Coulombic efficiencies of pristine and *in situ* grafted (deprotected) electrodes.

synthesis route. Differential capacity plots of the 10th cycle confirm this (Figure 6b).

Broadened and to lower potential shifted reduction peaks in the first cycle are also observed for nitrogen-containing amino and nitro groups (Figure 6c) what also intensifies in the 10th cycle (Figure 6d). However, for carboxy groups, the reduction peaks are slightly shifted to higher potentials and still very sharp. Even though those peaks deteriorate in the 10th cycle (Figure 6d), they are more pronounced than those of amino and nitro electrodes. Due to multilayer formation, a high number of functional groups is available on the electrode surface, also it is very likely that the grafted layer is thicker than for the ethynyl groups. The resulting SEI film alters the lithium-ion transport, which intensifies over cycling (Figure 6d). Therefore, the results from Figure 6a–d affirm our assumptions made earlier for the capacity and efficiency decrease in Figure 1c–d and 3a–b.

For *in situ* grafted samples, all reduction peaks in the first cycle are sharp and shifted to higher potentials, except amino (Figure 6e). The reduction peaks of amino are broadened and shifted to lower potentials in the first cycle, whereas in the 10th cycle just a flat line is observed, since amino does not deliver any capacity at this point anymore (Figure 6f). For the other samples even at the 10th cycle, the reduction peaks are preserved unlike for electrografted samples. Lithium-ion transport is even enhanced for ethynyl (TMS), given the sharp peaks which are shifted to lower/higher potentials during reduction/oxidation, respectively. Although, *in situ* grafting does not prevent multilayer formation, the grafted layer is not as dense and thick as it is for electrografted samples, which seems to have a positive impact on lithium-ion transport. However, the performance of carboxy and nitro electrodes still is inferior to the pristine at low and high current. Additional surface analysis is needed for a deeper understanding of the effect originating from the *in situ* grafted functional groups. However, Figure 6 reveals that the more the EC reduction peak is suppressed, the more the lithium-ion transport is negatively affected at low and high rate. This concerns especially the electrografted samples,

whereas the *in situ* grafted samples show defined EC reduction peaks and better lithium-ion transport at low and high rate. These findings correlate with the observed capacity values of all samples.

These results reveal that the grafting process highly influences the electrochemical performance of the functionalized electrodes. A main difference between the two grafting methods is that during *in situ* grafting solely the active material graphite is modified, whereas during electrografting the conductive additive and even the binder are impaired. The observation of binder degradation caused by side reactions with the deprotection agent reinforces this assumption. The combination of possible grafting on inactive materials (conductive additive and binder) and dense multilayer formation (as discussed earlier) seems to have a bad impact on the electrode-electrolyte interface and result in poorer performance. As stated by Shodiev *et al.*,^[25] the porosity and pore network organization have a great impact on the penetration of the electrode with electrolyte. By covering graphite and conductive additive with a thick functionalized layer, the penetration with electrolyte could be impaired and influence the SEI formation. Adhesion properties of the binder to the current collector and graphite could also be affected. However, additional analytic characterization is needed to investigate the resulting SEI properties.

Conclusions

Various functionalized aryl diazonium salts were used to successfully modify graphite electrodes *via* electro- and *in situ* grafting. In the case of alkyl silyl protected ethynyl aryl diazonium salts, the deprotection agent TBAF caused side reactions with PVdF as well as CMC/SBR binder. The resulting decomposition negatively affected the electrochemical performance of the modified electrodes for their application in LIBs. However, other functional groups such as amino, carboxy and nitro, for which no deprotection step is needed, show poor electrochemical performances as well. This was associated with

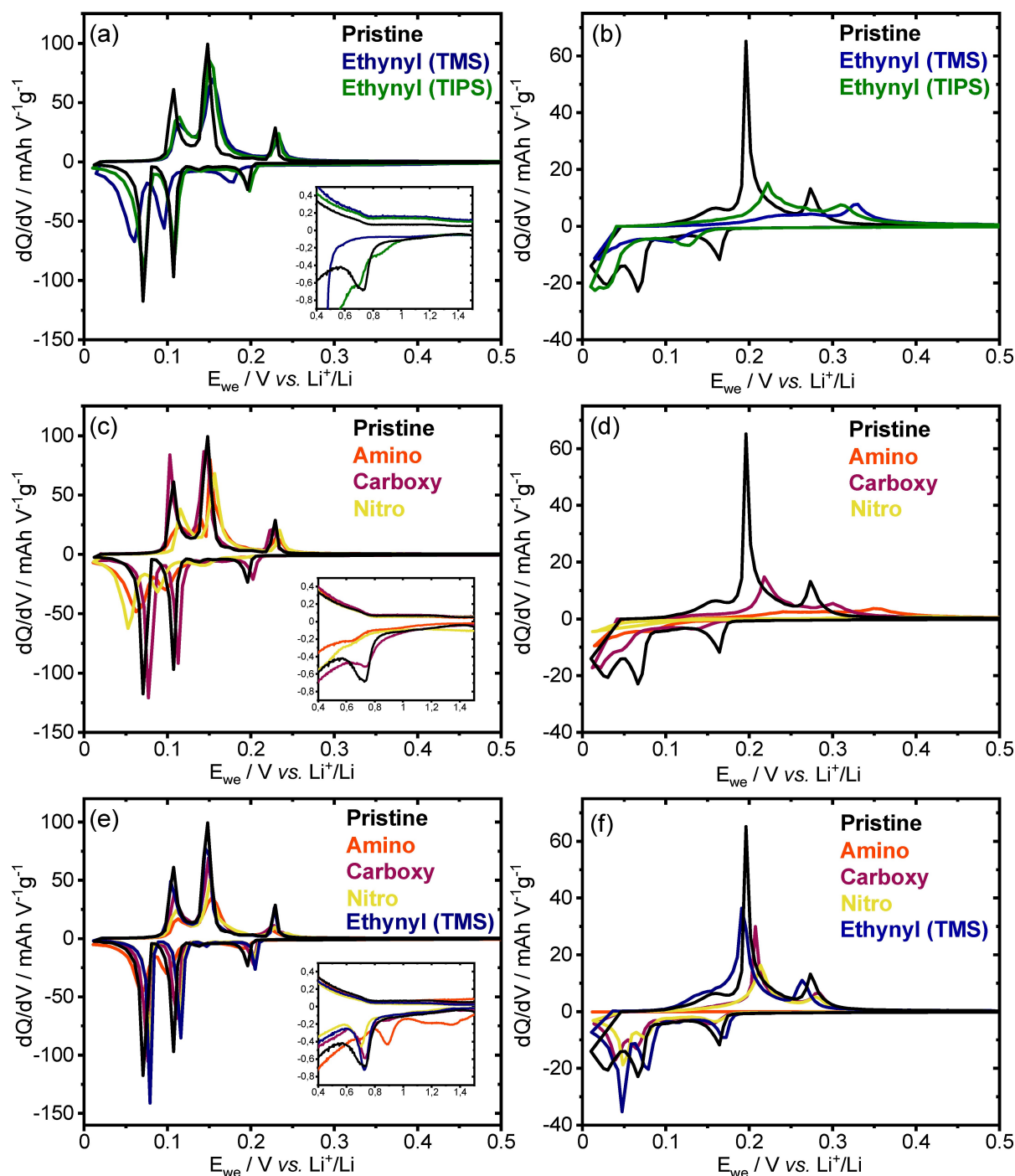


Figure 6. dQ/dV plots of the first and 10th cycle of pristine and (a), (b) electrografted ethynyl (TMS) and ethynyl (TIPS); (c), (d) electrografted electrodes amino, carboxy, nitro and (e), (f) *in situ* grafted amino, carboxy, nitro and ethynyl (TMS).

multilayer formation during electrografting. Therefore, *in situ* grafting was studied as an alternative technique. The *in situ* modified graphites show better electrochemical cycling performance, increased Coulombic efficiency in the first cycle and faster lithium-ion intercalation kinetics. Ethynyl (TMS) even increased the capacity to 238 mA h g⁻¹ at 1 C and shows capacity retention of 84% after 45 charge-discharge cycles, meaning more lithium-ions are available for (de)intercalation.

This work demonstrates that not only the functional group itself but also the method of formation must be considered to reveal the impact of functional groups at graphite electrodes for lithium-ion batteries. Concerning the introductory questions, we conclude that the hydrophilicity of the functional group does not determine the performance and a non-reducible group such as amino does not guarantee superior efficiencies. The preparation method, on the other hand, is of crucial

importance. Especially for the design of a covalent artificial SEI, the selection of eligible terminal groups and how several building blocks are included in the artificial network are of great significance. We provided insight into the design of suitable anchor groups *via* diazonium chemistry and the challenges of surface modification methods. Ethynyl groups offer good possibilities for post-functionalization *via* alkyne Click chemistry.^[11,32,33] The layered surface could be customized in terms of pore size and polarity to further improve SEI formation and lithium-ion (de)intercalation and help to reduce irreversible capacity loss.

Experimental Section

Electrode Preparation

90% w/w graphite (Mechano-Cap 1P1, H.C. Carbon) and 3% w/w conductive additive C65 (C-ENERGY) were pestled and dry-mixed at 1000 rpm in a speedmixer (DAC150.1 FVZ, Hauschild). Dimethyl sulfoxide (DMSO) was added dropwise, and the dispersion was mixed at different speeds between 1500 and 3000 rpm before 7% w/w polyvinylidene fluoride (PVdF) binder dissolved in DMSO was added. Mixing the dispersion for 10 min at 800 rpm gave a viscous paste that was subsequently coated on copper foil with a doctor blade (wet thickness 200 μm , dry thickness 120 $\mu\text{m} \pm 5 \mu\text{m}$). The coating was dried at room temperature overnight, at 120 °C for 8 h and finally at 120 °C in vacuum overnight.

Surface Modifications

Electrografting (on basis of [24] and [14])

All experiments were performed in an Ar-filled glovebox. Electrografting of ADS was performed in glass cells with rectangular cut pieces (approximately 15 × 35 mm) of pristine graphite electrodes as working electrode, a platinum mesh as counter electrode and Ag/AgNO₃ (0.1 M) as reference electrode. A solution of 0.1 M tetrabutylammonium tetrafluoroborate (TBATFB) in acetonitrile was used as electrolyte. To calibrate the reference electrode, platinum was used as working and counter electrode in a 1 mM solution of ferrocene. Cyclic voltammetry was performed for 5 cycles between −0.4 V and 0.4 V vs. Ag/AgNO₃ at a 20 mV/s scan rate.

General procedure for reductive electrografting of ADS

The corresponding aryl diazonium salt was dissolved in the electrolyte to receive a 0.01 M solution. A constant potential of −0.6 V vs. Ag/AgNO₃ was applied for 1 h to graft the aryl diazonium salt onto the graphite surface. After the grafting process, the working electrode was immersed in acetonitrile for 10 min and rinsed with acetonitrile to wash away any residues.

General procedure for in situ grafting of ADS (on basis of [26])

8.3 mmol of the corresponding aniline, 8.3 mmol sodium nitrite and, subsequently, 10 ml of concentrated hydrochloric acid were added to a dispersion of 1 g graphite in 50 ml water. After stirring overnight, the dispersion was filtered and washed thoroughly with water and acetone. For the deprotection of 4-[(Trimethylsilyl)ethynyl]benzenediazonium tetrafluoroborate the grafted powder was stirred in a solution of 0.1 M TBAF in THF for 30 min

before the deprotected powder was filtered and washed with THF. All powders were dried under vacuum and used for electrode preparation as described earlier.

General procedure for deprotection of grafted alkylsilyl protected ethynyl ADS

To deprotect the alkyne moiety of ADS, electrografted electrodes were immersed in a 0.1 M solution of tetrabutylammonium fluoride (TBAF) in tetrahydrofuran (THF) for 30 min with occasional swaying of the solution. Subsequently, the deprotected electrodes were immersed in THF for 10 min and rinsed with THF afterwards to wash away any residues. *In situ* grafted graphite powders were stirred in a solution of 0.1 M TBAF in THF for 30 min before the deprotected powder was filtered and washed with THF.

Cell Assembly

Electrochemical measurements were performed in a three-electrode setup in a custom-built polyether ether ketone (PEEK) cell with spring loaded titanium pistons as described in.^[34] Cell assembly was performed in an Ar-filled glovebox. Working electrodes and lithium metal counter electrodes were punched to 12 mm discs with a 13 mm glassfiber separator (GF/D, Whatman) in between. Lithium metal was used as reference electrode. The cells were filled with 1 M LiPF₆ in a 50:50 % v/v mixture of ethylene carbonate (EC) and dimethyl carbonate (DMC) electrolyte (LP30, BASF).

Electrochemical Measurements

All measurements were carried out in climate chambers at 25 °C using a VMP3 potentiostat (Biologic). Galvanostatic Cycling with Potential Limitation (GCPL) measurements were performed between 0.01 V and 1.80 V vs. Li⁺/Li with C/10 for 5 cycles followed by 45 cycles with 1 C.

Scanning Electron Microscopy

Scanning electron microscopy (SEM) measurements were conducted by a thermal field emission scanning electron microscope (FESEM, Carl Zeiss SMT AG) at an acceleration voltage of 5 kV. The samples were fixed on a steel sample holder by using sticky tape.

X-ray Photoelectron Spectroscopy

X-ray photoemission measurements were performed using a K-alpha or K-alpha⁺ XPS spectrometer from Thermo Fisher Scientific. The samples were illuminated with monochromatic Al-K _{α} X-rays with a spot size of about 400 μm . The photoelectrons were detected with a hemispherical 180 dual focus analyzer with 128 channel detectors. To prevent any localized charge buildup, the K-Alpha charge compensation system was employed during analysis, using electrons of 8 eV energy and low-energy argon ions. The Thermo Advantage software was used for data acquisition and processing.^[35] The spectra were fitted with one or more Voigt profiles (binding energy uncertainty: ± 0.2 eV). All spectra were referenced to the C 1s peak of hydrocarbon at 285.0 eV binding energy controlled by means of the well-known photoelectron peaks of metallic Cu, Ag, and Au.

Supporting Information

Additional data about synthesis, surface and electrochemical characterization.

Acknowledgements

This work contributes to the research performed at CELEST (Center for Electrochemical Energy Storage Ulm-Karlsruhe). We acknowledge the SFB 1176 funded by the German Research Foundation (DFG) in the context of project B2 for funding. M. B. thanks Dr. Günter Staufer and Dr. Mathias Widmaier for useful discussion and Dr. Raheleh Azmi for support with XPS measurements. H. R. thanks the Federal Ministry of Education and Research (BMBF) within the project Flow3DKat (03EK3053C) for financial support. Open Access funding enabled and organized by Projekt DEAL.

Conflict of Interest

The authors declare no conflict of interest.

Keywords: Aryl diazonium salts · Electrografting · Graphite · *In situ* grafting · Lithium-ion batteries · Surface groups

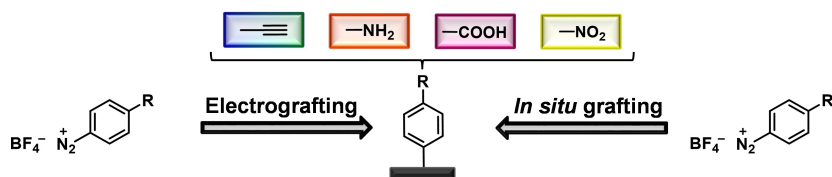
- [1] H. Zhang, Y. Yang, D. Ren, L. Wang, X. He, *Energy Storage Mater.* **2021**, *36*, 147–170.
- [2] W. Qi, J. G. Shapter, Q. Wu, T. Yin, G. Gao, D. Cui, *J. Mater. Chem. A* **2017**, *5*, 19521–19540.
- [3] J. Asenbauer, T. Eisenmann, M. Kuenzel, A. Kazzazi, Z. Chen, D. Bresser, *Sustain. Energy Fuels* **2020**, *5*, 5387–5416.
- [4] P. G. Kitz, P. Novák, E. J. Berg, *ACS Appl. Mater. Interfaces* **2020**, *12*, 15934–15942.
- [5] L. J. Fu, H. Liu, C. Li, Y. P. Wu, E. Rahm, R. Holze, H. Q. Wu, *Solid State Sci.* **2006**, *8*, 113–128.
- [6] G. Liu, J. Liu, T. Böcking, P. K. Eggers, J. J. Gooding, *Chem. Phys.* **2005**, *319*, 136–146.
- [7] M. Sandomierski, A. Voelkel, *J. Inorg. Organomet. Polym. Mater.* **2021**, *31*, 1–21.
- [8] M. M. Chehimi, A. Lamouri, M. Picot, J. Pinson, *J. Mater. Chem. C* **2014**, *2*, 356–363.
- [9] A. A. Mohamed, Z. Salmi, S. A. Dahoumane, A. Mekki, B. Carbonnier, M. M. Chehimi, *Adv. Colloid Interface Sci.* **2015**, *225*, 16–36.
- [10] N. Delaporte, G. Lajoie, S. Collin-Martin, K. Zaghbi, *Sci. Rep.* **2020**, *10*, 3812.
- [11] T. Wu, C. M. Fitchett, P. A. Brooksby, A. J. Downard, *ACS Appl. Mater. Interfaces* **2021**, *13*, 11545–11570.
- [12] H. Saneifar, D. Bélanger, *J. Solid State Electrochem.* **2021**, *25*, 149–158.
- [13] Y. R. Leroux, P. Hapiot, *Chem. Mater.* **2013**, *25*, 489–495.
- [14] D. S. Moock, S. O. Steinmüller, I. D. Wessely, A. Llevot, B. Bitterer, M. A. R. Meier, S. Bräse, H. Ehrenberg, F. Scheiba, *ACS Appl. Mater. Interfaces* **2018**, *10*, 24172–24180.
- [15] Q. Pan, H. Wang, Y. Jiang, *J. Mater. Chem.* **2007**, *17*, 329–334.
- [16] P. Verma, P. Novák, *Carbon* **2012**, *7*, 2599–2614.
- [17] M. E. Spahr, in *Lithium-Ion Batteries*, 1st ed., M. Yoshio, R. J. Brodd, A. Kozawa, Eds. New York: Springer, **2009**, 117–154.
- [18] M. Widmaier, N. Jäckel, M. Zeiger, M. Abuzarli, C. Engel, L. Bommer, V. Presser, *Electrochim. Acta* **2017**, *247*, 1006–1018.
- [19] M. E. Spahr, D. Goers, A. Leone, S. Stallone, E. Grivei, *J. Power Sources* **2011**, *196*, 3404–3413.
- [20] K. Pfeifer, S. Arnold, Ö. Budak, X. Luo, V. Presser, H. Ehrenberg, S. Dsoke, *J. Mater. Chem. A* **2020**, *8*, 6092–6104.
- [21] N. Shpigel, M. D. Levi, S. Sigalov, O. Girshevit, D. Aurbach, L. Daikhin, N. Jäckel, V. Presser, *Angew. Chem.* **2015**, *127*, 12530–12533; *Angew. Chem. Int. Ed.* **2015**, *54*, 12353–12356.
- [22] Y. Zhu, J. Wang, F. Zhang, S. Gao, A. Wang, W. Fang, J. Jin, *Adv. Funct. Mater.* **2018**, *28*, 1804121.
- [23] X. Zheng, R. D. Gandour, K. J. Edgar, *Biomacromolecules* **2013**, *14*, 1388–1394.
- [24] T. Menanteau, M. Dias, E. Levillain, A. J. Downard, T. Breton, *J. Phys. Chem. C* **2016**, *120*, 4423–4429.
- [25] A. Shodiev, E. Primo, O. Arcelus, M. Chouchane, M. Osenberg, A. Hilder, I. Manke, J. Li, A. A. Franco, *Energy Storage Mater.* **2021**, *38*, 80–92.
- [26] C. Martin, M. Alias, F. Christien, O. Crosnier, D. Bélanger, T. Brousse, *Adv. Mater.* **2009**, *21*, 4735–4741.
- [27] S. Kesavan, S. A. John, *RSC Adv.* **2016**, *6*, 62876–62883.
- [28] G. Ambrosio, G. Drera, G. Di Santo, L. Petaccia, L. Daukiya, A. Brown, B. Hrisch, S. De Feyter, L. Sangaletti, S. Pagliara, *Sci. Rep.* **2020**, *10*, 4114.
- [29] S. J. An, J. Li, C. Daniel, D. Mohanty, S. Nagpure, D. L. Wood III, *Carbon* **2016**, *105*, 52–76.
- [30] R. Imhof, P. Novák, *J. Electrochem. Soc.* **1998**, *145*, 1081–1087.
- [31] S. S. Zhang, *J. Power Sources* **2006**, *162*, 1379–1394.
- [32] M. Bengamra, A. Khelifi, N. Ktari, S. Mahouche-Chergui, B. Carbonnier, N. Fourati, R. Kalfat, M. M. Chehimi, *Langmuir* **2015**, *31*, 10717–10724.
- [33] O. Gusebnikova, V. Svorcik, O. Lyutakov, M. M. Chehimi, P. S. Postnikov, *Sensors* **2019**, *19*, 2110.
- [34] D. Weingarth, M. Zeiger, N. Jäckel, M. Aslan, G. Feng, V. Presser, *Adv. Energy Mater.* **2014**, *4*, 1400316.
- [35] K. L. Parry, A. G. Shard, R. D. Short, R. G. White, J. D. Whittle, A. Wright, *Surf. Interface Anal.* **2006**, *38*, 1497–1504.

Manuscript received: October 21, 2021

Revised manuscript received: December 6, 2021

Accepted manuscript online: December 7, 2021

RESEARCH ARTICLE



A matter of modification: Aryl diazonium salts are used to functionalize graphite electrodes for lithium-ion batteries. Surface modification of graphite electrodes with ethynyl, amino, carboxy and nitro groups *via* electro- and *in situ* grafting shows that not only the functional group but

also the modification method plays an important role when it comes to their electrochemical performance. Other electrode components, such as the binder, can be affected during the modification process, leading to a deterioration of the electrochemical performance.

M. Bauer, Dr. K. Pfeifer, X. Luo, H. Radinger, Prof. Dr. H. Ehrenberg, Dr. F. Scheiba*

1 – 12

Functionalization of Graphite Electrodes with Aryl Diazonium Salts for Lithium-Ion Batteries

